Retrieval of volcanic and man-made stratospheric aerosols from orbital polarimetric measurements

MICHAEL I. MISHCHENKO,[1,*] JANNA M. DLUGACH,[2] ANDREW A. LACIS,[1] LARRY D. TRAVIS,[1] AND BRIAN CAIRNS[1]

[1]*NASA Goddard Institute for Space Studies, 2880 Broadway, New York, NY 10025, USA*
[2]*Main Astronomical Observatory, National Academy of Sciences of Ukraine, 27 Zabolotny Str. 03680, Kyiv, Ukraine*
[*]*michael.i.mishchenko@nasa.gov*

Abstract: Stratospheric aerosols that are caused by a major volcanic eruption can serve as a valuable test of global climate models, as well as severely complicate tropospheric-aerosol monitoring from space. In either case, it is highly desirable to have accurate global information on the optical thickness, size, and composition of volcanic aerosols. We report sensitivity study results, which analyze the implications of making precise multi-angle photopolarimetric measurements in a 1.378-μm spectral channel residing within a strong water-vapor absorption band. We demonstrate that, under favorable conditions, such measurements would enable near-perfect retrievals of the optical thickness, effective radius, and refractive index of stratospheric aerosols. Besides enabling accurate retrievals of volcanic aerosols, such measurements can also be used to monitor man-made particulates injected in the stratosphere for geoengineering purposes.

1. Introduction

While the typical background value of the optical thickness of stratospheric aerosols is very small, aerosol layers caused by major volcanic eruptions can be optically much thicker and can have a significant short-term climate impact [1,2]. As such, volcanic aerosols can represent an extremely valuable natural experiment ideally suited for testing climate models provided that the global distribution of all relevant aerosol properties is accurately determined from orbital observations [3,4]. At the same time, the drastic appearance of an optically thick layer of stratospheric aerosols can represent a major challenge for satellite instruments intended for long-term monitoring of tropospheric aerosols. Therefore, an aerosol monitoring space mission should have a built-in capacity to retrieve stratospheric aerosols independently of tropospheric aerosols since this information is critical for the subsequent tropospheric-aerosol retrieval.

Besides the potentially massive contribution from a major volcanic eruption, another source of stratospheric aerosols could be the implementation of climate geoengineering programs increasingly discussed in the literature [5]. Obviously, the capability to perform global and accurate monitoring of man-made stratospheric particulates must be an indispensable part of geoengineering programs based on stratospheric aerosol injection.

One can think of various ways of inferring the properties of stratospheric aerosols from independent satellite observations, e.g., by using occultation or limb scatter measurements [6–8]. However, such retrievals do not yield simultaneous stratospheric-aerosol properties within the field of view of the instrument used for monitoring tropospheric aerosols. Furthermore, they may not yield all the requisite particle microphysics needed for climate modeling and tropospheric-aerosol retrievals. It would thus be decidedly preferable to endow the same orbital tropospheric-aerosol instrument with the capacity to independently retrieve the

requisite properties of stratospheric aerosols (such as their optical thickness, size distribution, and composition).

The critical importance of satellite polarimetry for global monitoring of tropospheric aerosols was first articulated in the late 1980s and early 1990s [9,10]. Since then passive polarimeters have come to be recognized as an indispensable part of any advanced orbital mission intended for accurate global retrievals of detailed properties of tropospheric aerosols [11–16]. Therefore, the main objective of this paper is to discuss a straightforward way of isolating stratospheric aerosols in passive photopolarimetry by using observations in the strong 1.378-μm water-vapor absorption band [17]. We will describe a sensitivity study illustrating the capacity of a high-precision multi-angle polarimeter to yield the requisite stratospheric-aerosol properties in favorable circumstances as well as discuss what help the polarimeter may need in more challenging situations.

2. Basic assumptions

Let us assume that an orbital photopolarimeter is equipped with a narrow spectral channel centered at 1.378 μm. Following [17], we define the favorable observation conditions as follows:

(i) the amount of water vapor in the troposphere is sufficiently large that strong absorption in the 1.378-μm water-vapor band extinguishes any contribution of the surface, tropospheric aerosols, and liquid-water clouds to the outgoing radiation detected by the satellite instrument; and

(ii) cirrus clouds are absent in the instrument's field of view.

Then everything the orbital instrument "sees" is an isolated layer of stratospheric aerosols without a reflecting bottom boundary. We will further assume that

(iii) the stratospheric aerosols are homogeneous spherical particles (e.g., dominated by H_2SO_4/H_2O aerosols) having the same chemical composition and characterized by a monomodal size distribution.

Following [18–20] as a template, the essence of our sensitivity study is to model theoretically the photopolarimetric signal carried by the sunlight diffusely reflected by stratospheric aerosols; add realistic measurement errors to this signal; and verify whether a multi-angle orbital photopolarimeter would have the capacity to retrieve the requisite aerosol parameters from this simulated error-laden measurement.

3. Numerical technique

In radiative transfer computations, we use the standard geometric and polarimetric conventions [18,21,22]. The stratosphere is illuminated by a parallel unpolarized beam of sunlight incident in the direction $\{\theta_0, \varphi_0\}$, where $90° \le \theta_0 \le 180°$ is the solar zenith angle and φ_0 is the solar azimuth angle. The photopolarimetric state of the light diffusely reflected in the satellite direction $\{0° \le \theta \le 90°, \varphi\}$ is defined as a real-valued four-element specific intensity column vector having the Stokes parameters as its components:

$$\mathbf{I}(\theta,\varphi) = \begin{bmatrix} I(\theta,\varphi) \\ Q(\theta,\varphi) \\ U(\theta,\varphi) \\ V(\theta,\varphi) \end{bmatrix}. \qquad (1)$$

We will assume, as usual, that the fourth Stokes parameter carries little useful information [23] and is not measured. We then have

$$I(\theta,\varphi) = \mu_0 R_{11}(\tau_0,\mu,\mu_0,\varphi-\varphi_0)F_0, \tag{2}$$

$$Q(\theta,\varphi) = \mu_0 R_{21}(\tau_0,\mu,\mu_0,\varphi-\varphi_0)F_0, \tag{3}$$

$$U(\theta,\varphi) = \mu_0 R_{31}(\tau_0,\mu,\mu_0,\varphi-\varphi_0)F_0, \tag{4}$$

where $\mu = \cos\theta$, $\mu_0 = -\cos\theta_0$, τ_0 is the optical thickness of the stratospheric aerosol layer, $\mathbf{R}(\tau_0,\mu,\mu_0,\varphi-\varphi_0)$ is the 4×4 so-called reflection matrix with real-valued components, and πF_0 is the incident electromagnetic energy flux per unit area perpendicular to the solar beam. Note that the reflection matrix relates the Stokes parameters of the incident and scattered light defined with respect to their individual meridional planes. Since the scattering medium is assumed to consist of spherical (or randomly oriented nonspherical) particles, the reflection matrix depends on the difference between the azimuth angles of the reflected and incident beams rather than on their individual values. Instead of $Q(\theta,\varphi)$ and $U(\theta,\varphi)$, in what follows we use the normalized Stokes parameters

$$q(\theta,\varphi) = \frac{Q(\theta,\varphi)}{I(\theta,\varphi)} \text{ and } u(\theta,\varphi) = \frac{U(\theta,\varphi)}{I(\theta,\varphi)}. \tag{5}$$

To compute $\mathbf{R}(\tau_0,\mu,\mu_0,\varphi-\varphi_0)$, we use the so-called fast invariant-imbedding technique. This numerically-exact solver of the vector radiative transfer equation is described in [24]. The requisite single-scattering input is calculated using the Lorenz–Mie program described in [25]. We assume the standard gamma distribution of particle radii [25,26] given by

$$n(r) = \text{constant}\times r^{(1-3v_{\text{eff}})/v_{\text{eff}}}\exp\left(-\frac{r}{r_{\text{eff}}v_{\text{eff}}}\right), \tag{6}$$

where $n(r)\mathrm{d}r$ is the fraction of particles with radii from r to $r+\mathrm{d}r$, r_{eff} and v_{eff} are the effective radius and effective variance of the size distribution, respectively, and the constant ensures proper normalization. Throughout this paper, the effective variance is fixed at a moderate value $v_{\text{eff}} = 0.15$ representing size distributions that are neither too narrow nor too wide. The wavelength is fixed at 1.378 μm.

4. Sensitivity analysis

To simulate multi-angle satellite observations, we fix μ_0 at 0.6 and assume that the cosine of the satellite zenith angle varies from $\mu = 0.2$ to $\mu = 1$ in steps of 0.2 in the azimuthal planes corresponding to $\varphi-\varphi_0 = 60°$ and $\varphi-\varphi_0 = -120°$. We thus have nine observation geometries covering the scattering-angle range 74°–136°.

To simulate the retrieval of aerosol properties from photometric, polarimetric, and photopolarimetric observations, respectively, we use three "acceptance" criteria (A), (B), and (C), as follows:

$$\text{(A):}\quad \frac{1}{9}\sum_{j=1}^{9}\frac{\left|I_{\text{c}}^{j}-I_{\text{s}}^{j}\right|}{I_{\text{s}}^{j}} \le \varepsilon_I, \tag{7}$$

$$\text{(B):}\quad \frac{1}{9}\sum_{j=1}^{9}\frac{1}{2}\left(\left|q_{\text{c}}^{j}-q_{\text{s}}^{j}\right|+\left|u_{\text{c}}^{j}-u_{\text{s}}^{j}\right|\right) \le \varepsilon_P, \tag{8}$$

$$\text{(C)} = \text{(A)} \wedge \text{(B)}. \tag{9}$$

Here, j numbers the observation geometries; "s" labels the specific intensities (radiances) and normalized Stokes parameters computed for a "standard" aerosol model representing the "actual" aerosol population; "c" labels the same quantities computed for a "candidate" aerosol model; ε_I is the relative accuracy of intensity measurements; and ε_P is the polarimetric accuracy, i.e., the absolute accuracy of measuring the normalized Stokes parameters q and u. The meaning of these criteria is clear: all candidate models that satisfy criterion (A) form the set of equally acceptable aerosol models retrieved from simulated error-laden intensity-only measurements for the actual aerosol population; criterion (B) applies to polarization-only measurements; and criterion (C) is the superposition of criteria (A) and (B) applicable to the combined use of photometric and polarimetric data. In what follows, the radiometric accuracy ε_I will be fixed at a rather typical value of 0.04. With one explicit exception, the assumed polarimetric uncertainty will be $\varepsilon_P = 0.002$. Both accuracies are characteristic of a high-precision instrument such as the NASA's Aerosol Polarimetry Sensor (APS) [12,27].

Let us first assume that the refractive index of stratospheric aerosols is known beforehand and is equal to m = 1.42, thereby being representative of H_2SO_4/H_2O particles at the wavelength considered. We define three standard aerosol models as those given by $\tau_{0,s} = 0.1$ and $r_{\mathrm{eff,s}} = 0.45,\ 0.5$, and 0.55 μm. Such values are quite typical of evolved volcanic aerosols [4]. The effective radii of candidate models vary from 0.4 to 0.6 μm, while their optical thicknesses vary from 0 to 0.2.

The results of applying criteria (A), (B), and (C) to all candidate models are shown by the left-hand, middle, and right-hand columns of Fig. 1, respectively. The top, middle, and bottom rows of panels correspond to $r_{\mathrm{eff,s}} = 0.45,\ 0.5$, and 0.55 μm, so that the intersection of the vertical and horizontal dashed lines defines the respective standard model. The green areas in the left-hand and middle columns show the corresponding ranges of acceptable candidate models, while the right-hand column shows the intersection of these areas representing the application of criterion (C).

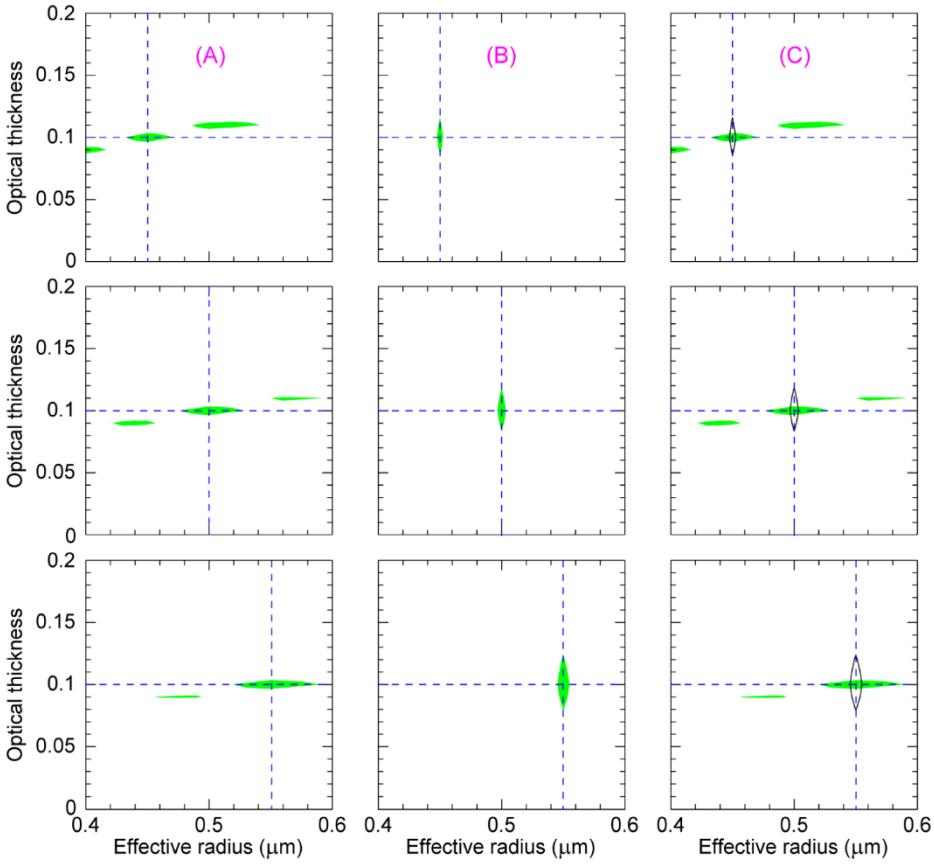

Fig. 1. Simultaneous retrieval of the optical thickness and effective radius for three standard aerosol models with the same *a priori* known refractive index $m = 1.42$.

It is seen that the combined use of photomertric and polarimetric observations (the right-hand column of diagrams) enables one to retrieve both τ_0 and r_{eff} with exquisite accuracy. The high accuracy of retrieving the effective radius is fully defined by the use of polarimetry (the middle column), while intensity-only measurements (the left-hand column) have poor size sensitivity and can therefore yield inaccurate estimates of the total particle volume (or mass).

Interestingly, however, photometric observations alone can be used to retrieve the aerosol optical thickness with accuracy comparable to (if not finer than) that of polarimetric-only retrievals. This can be explained by the fact that $\tau_{0,s} = 0.1$ is small enough to approximately yield the single-scattering regime of radiative transfer:

$$\mathbf{R}(\tau_0, \mu, \mu_0, \varphi - \varphi_0) \underset{\tau_0 \to 0}{=} \frac{\varpi \tau_0}{4\mu\mu_0} \tilde{\mathbf{Z}}(\theta, \theta_0, \varphi - \varphi_0), \tag{10}$$

where ϖ is the single-scattering albedo and $\tilde{\mathbf{Z}}(\theta, \theta_0, \varphi - \varphi_0)$ is the (normalized) Stokes phase matrix [21]. As a consequence, the normalized Stokes parameters $q(\theta, \varphi)$ and $u(\theta, \varphi)$ are weakly dependent on (and hence have reduced sensitivity to) τ_0.

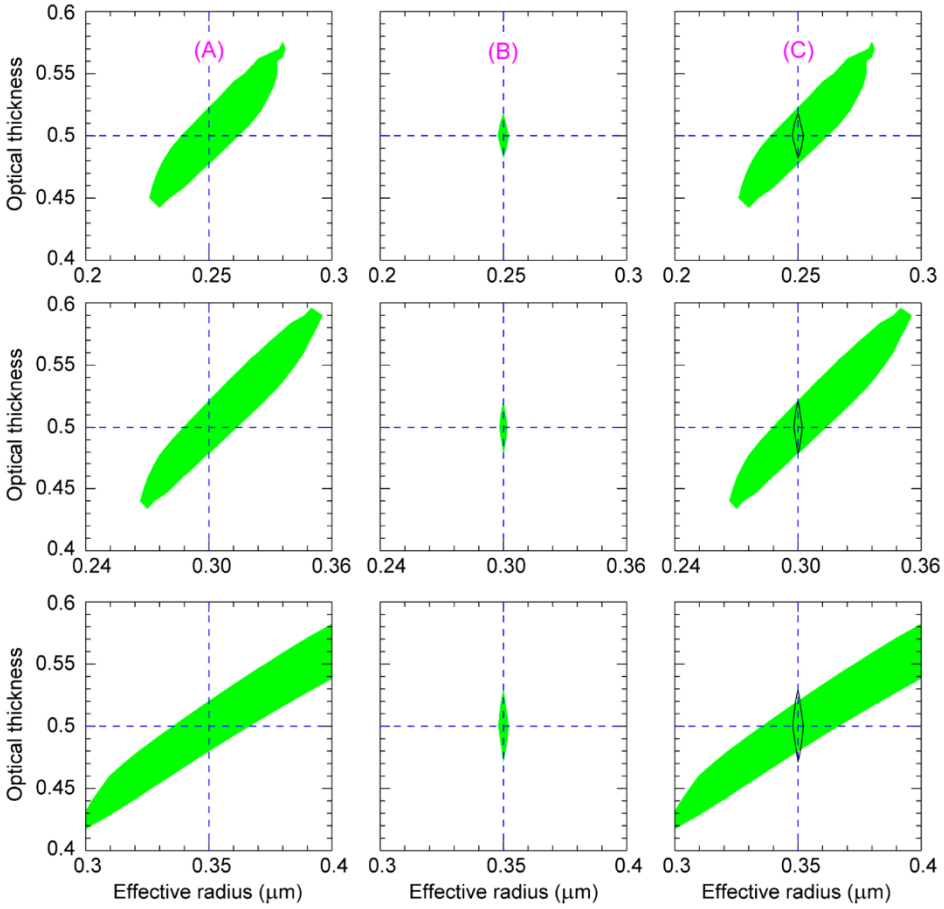

Fig. 2. As in Fig. 1 but for $\tau_{0,s} = 0.5$ and $r_{\text{eff,s}} = 0.25,$ 0.3, and 0.35 μm.

This explanation implies that as $\tau_{0,s}$ grows, the polarimetric-only retrieval can be expected to become increasingly sensitive to the optical thickness. This is illustrated in Fig. 2 computed for $\tau_{0,s} = 0.5$ and $r_{\text{eff,s}} = 0.25,$ 0.3, and 0.35 μm. Note that this value of $\tau_{0,s}$ and the particle size range may represent the extreme case of a locally thick freshly formed aerosol plume [4]. It can be seen that now the relative accuracy of the optical thickness retrieval in the middle bottom diagram is better than 6%. This accuracy can even be slightly improved by invoking radiometric measurements. The accuracy of the polarimetric-only retrieval of the effective radius is still exceptional. At the same time, the accuracy of the radiance-only retrieval of the optical thickness and effective radius has deteriorated to the point of becoming utterly unacceptable. Note that this conclusion is also valid for the effective radii used in Fig. 1.

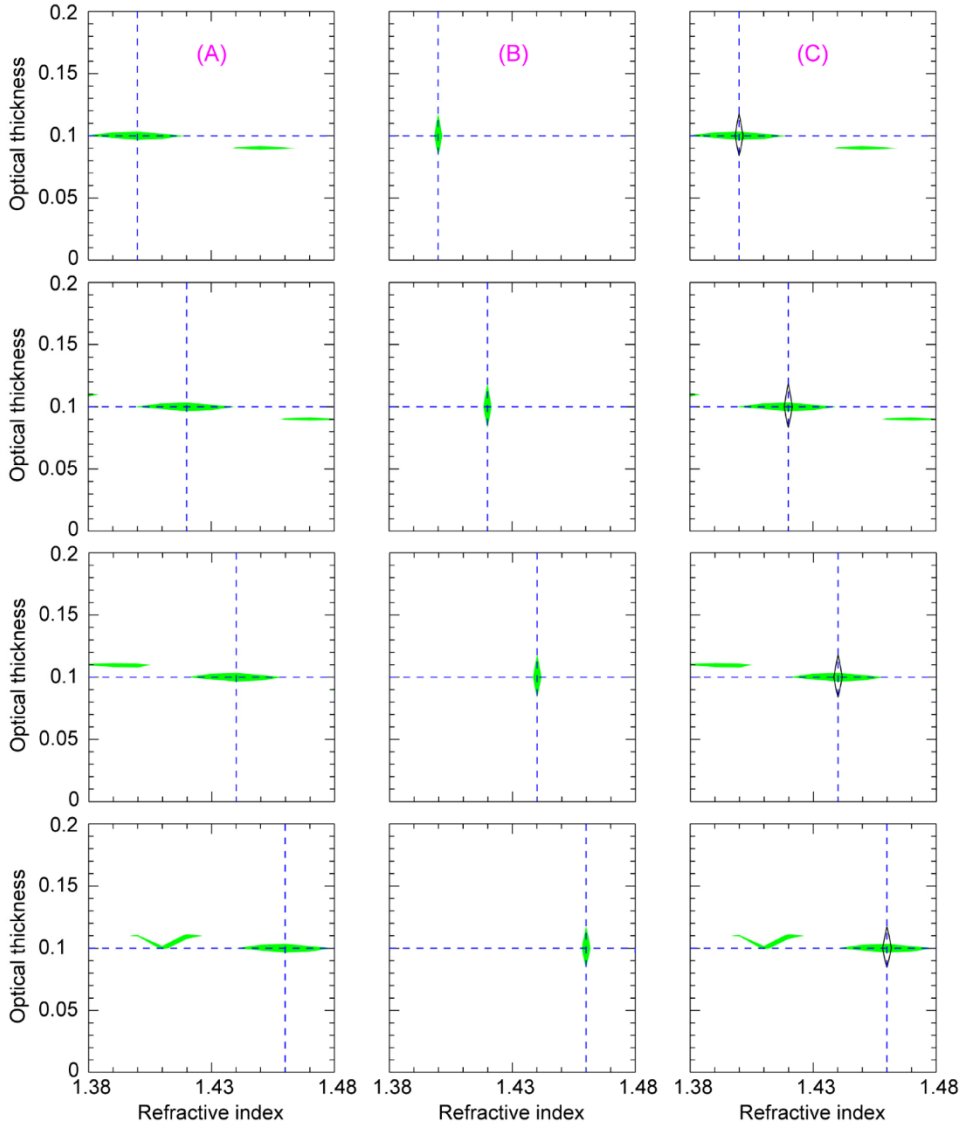

Fig. 3. Simultaneous retrieval of the optical thickness and refractive index for four standard aerosol models with the same *a priori* known effective radius $r_{\text{eff,s}} = 0.5$ μm.

Figure 3 parallels Fig. 1, except that now we assume that the effective radius of stratospheric aerosols is known beforehand and is $r_{\text{eff,s}} = 0.5$ μm, while the refractive indices of the standard models are $m_s = 1.4$, 1.42, 1.44, and 1.46. As before, the standard-model optical thickness is fixed at $\tau_{0,s} = 0.1$. It is seen again that the intensity-only retrieval of m is highly uncertain. However, the polarimetric-only retrieval of the refractive index and the combined ptotopolarimetric retrieval of τ_0 are nearly perfect.

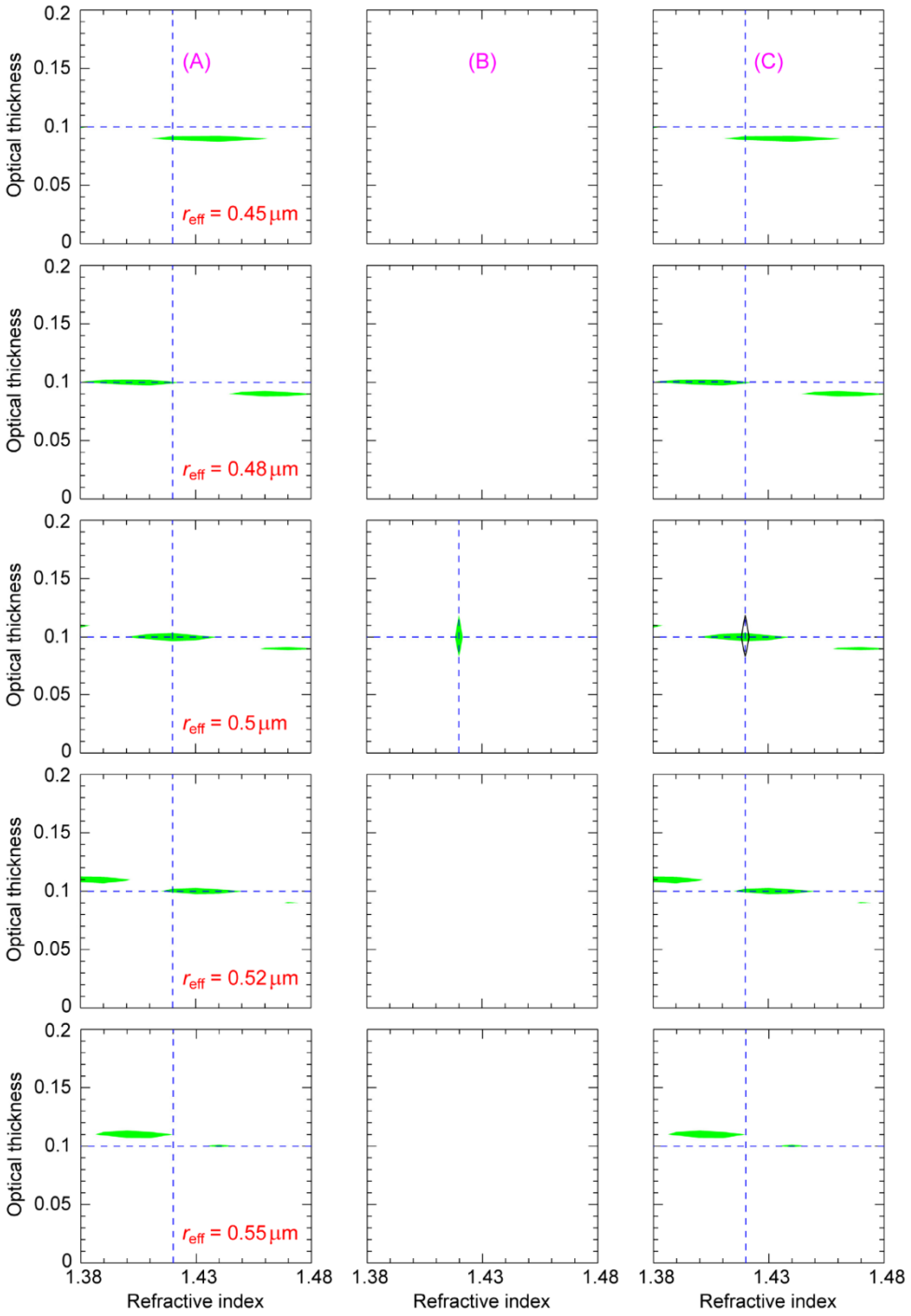

Fig. 4. Simultaneous retrieval of all three aerosol parameters.

The most challenging test is to assume that all three aerosol parameters are unknown and must be retrieved simultaneously. In this case the standard model is represented by $\tau_{0,s} = 0.1$, $m_s = 1.42$, and $r_{eff,s} = 0.5$ μm. Figure 4 demonstrates the performance of all three types of

retrieval algorithm by displaying results for candidate models with optical thicknesses ranging from 0 to 0.2, refractive indices ranging from 1.38 to 1.48, and effective radii $r_{\mathrm{eff,c}}$ = 0.45, 0.48, 0.5, 0.52, and 0.55 μm. The intersection of the dashed lines in the middle diagram for $r_{\mathrm{eff}} = 0.5$ μm corresponds to the correct solution.

It is seen that the polarimetric-only retrieval (the middle column of diagrams) yields a nearly perfect value of the refractive index and constrains the effective radius to better than ± 0.02 μm. Indeed, the fit for polarization is so restrictive that all the middle-column diagrams but one have no green areas showing acceptable candidate models. Furthermore, combining polarization and radiance data results in an exceedingly accurate optical thickness retrieval. At the same time, the intensity-only retrieval results in overly wide ranges of equally acceptable refractive-index and effective-radius values.

Finally, Fig. 5 demonstrates the importance of high polarimetric accuracy. It parallels Fig. 4, but is computed assuming that ε_P is 0.015 rather than 0.002. The former value may be characteristic of some types of polarimeter such as the Polarization and Directionality of the Earth's Reflectance instrument [28]. While the left-hand diagrams are the same as in Fig. 4, the middle-column diagrams exhibit dramatically expanded areas of acceptable candidate models for the polarization-only retrieval. The right-hand diagrams show that the optical-thickness accuracy remains meaningful, whereas the retrieval of the refractive index and effective radius becomes rather poorly constrained.

5. Discussion and conclusions

The results of the preceding section confirm that in favorable circumstances defined by assumptions (i)–(iii) in Section 2, a high-precision multi-angle photopolarimeter has the capacity to yield the optical thickness, size distribution, and refractive index of stratospheric aerosols with exceedingly high accuracy by making 1.378-μm observations. This undoubtedly is a direct consequence of single-scattering polarization being a very sensitive function of particle size, composition, and scattering geometry, as analyzed extensively in [18,25,26]. It is important, however, to discuss various complicating factors that can be encountered in practice.

Firstly, the amount of water vapor in the troposphere may be insufficient to extinguish the contributions from the surface, liquid-water clouds, and tropospheric aerosols to the scattered electromagnetic radiation reaching the orbital instrument. It is therefore essential to be able to reject such "contaminated" pixels. This can be achieved, for example, by having a 0.910-μm spectral channel providing independent information on the water vapor amount [29].

Secondly, depending on the age of stratospheric aerosols, they can be a mixture of two or more components with different size distributions and refractive indices. Although the likelihood of such a scenario decreases with aerosol age, it remains to be seen if high-accuracy multi-angle photopolarimetric measurements can still yield the requisite parameters of such a multimodal population. Achieving this may require, for example, the use of more than nine viewing directions discussed in this paper.

Thirdly, it is not inconceivable that at a certain stage in their evolution stratospheric aerosols can be at least partly nonspherical (e.g., dominated by volcanic ash particles). An unequivocal indication of nonsphericity would be nonzero backscattering depolarization measured by a lidar [22,25]. Such nonzero (and sometimes substantial) values of the linear depolarization ratio have been reported [30–38]. Yet the deviation from zero has often been a few percent or less, especially for evolved stratospheric aerosols presumably dominated by sulfuric-acid particles. Such small values suggest that the model of spherical scatterers is likely to be generally applicable. However, flying the polarimeter along with a polarization lidar (either elastic of high spectral resolution) can be expected to benefit polarimetric retrievals, and vice versa. There have been profound developments in the theory of light

scattering [39–41] that can potentially be used in retrieval algorithms explicitly taking into account nonsphericity of aerosol particles such as volcanic ash.

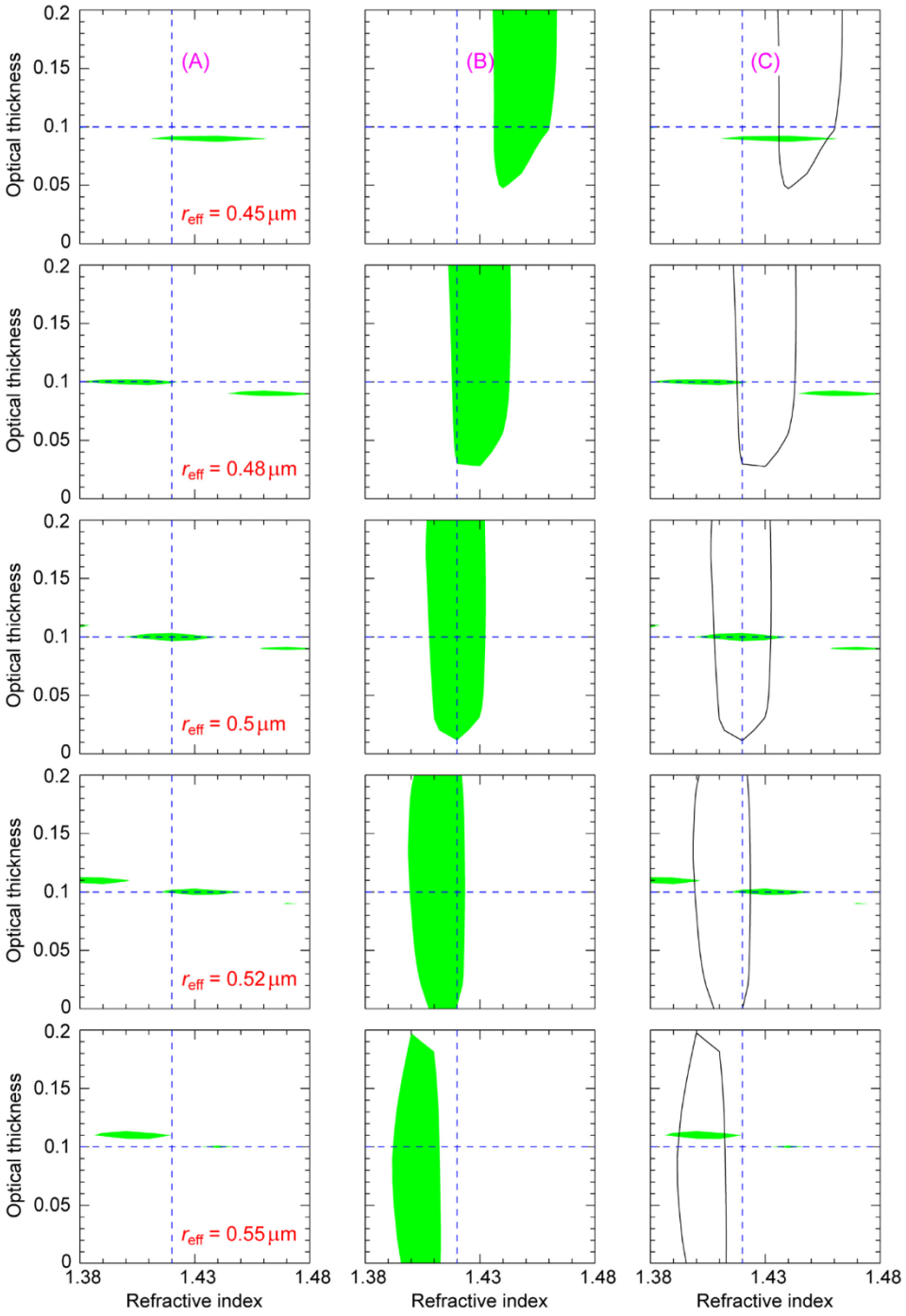

Fig. 5. As in Fig. 4, but for $\varepsilon_P = 0.015$.

Fourthly, the satellite field of view can capture an optically thick cirrus cloud, in which case the retrieval of both stratospheric aerosols and cirrus cloud particles from 1.378-µm

photopolarimetry alone may be problematic. Again, parallel lidar observations could help identify and discard cirrus-contaminated pixels. Since the spatial distribution of evolved volcanic aerosols is less heterogeneous than that of cirrus clouds, the loss of cirrus-contaminated pixels is unlikely to represent a major problem for the global monitoring of stratospheric particles.

The possibility of aerosol retrievals in situations with cirrus beneath the stratospheric aerosols, perhaps with and without the use of lidar data, needs to be further analyzed. While total intensities recorded by the orbital photopolarimeter would be substantially impacted by cirrus, the second and third Stokes parameters, Q and U, would be much less affected as cirrus are among the least polarizing natural objects [42]. In contrast, stratospheric aerosols are quasi-Rayleigh like at 1.378 μm, with the variation of Q and U at side scattering angles being sensitive to size, and it might still be possible therefore to retrieve useful information on their size and optical thickness.

In summary, endowing a high-precision multi-angle orbital photopolarimeter with a 1.378-μm channel (in combination with a 0.910-μm channel) is highly desirable (if not mandatory) from the perspective of monitoring volcanic stratospheric aerosols and their climate impact. Potentially small radiance levels and stringent accuracy requirements may necessitate having on-board radiance and polarimetric calibration. A good example would be the NASA's APS [12,27] (see also [43]). Using the 1.378-μm channel to determine the requisite properties of stratospheric aerosols can be expected to substantially improve the subsequent retrieval of tropospheric aerosols using photopolarimetric observations in other spectral channels.

Finally, stratospheric aerosol geoengineering has increasingly been discussed as a means of addressing the global-warming problem [5,44–47]. Should a decision be ever made to attempt geoengineering with stratospheric aerosols, a high-precision multi-angle photopolarimeter equipped with a 1.378-μm channel would provide the critical capacity to monitor detailed and global properties of such man-made particulates. The optimal material of artificial stratospheric aerosols has been the subject of debate [48–50], and the corresponding refractive index may differ substantially from that of volcanic stratospheric aerosols. Then, again, the simultaneous retrieval of the requisite parameters of both natural and man-made particulates may require photopolarimetric measurements at an increased number of scattering angles.

Funding

National Aeronautics and Space Administration (NASA) Radiation Sciences Program, NASA ACE Program, and NASA Remote Sensing Theory Program. Comprehensive Program for Space Research of the National Academy of Sciences of Ukraine for 2018–2022.

Acknowledgments

We thank Nadia Zakharova for providing Figs. 1–5 and two anonymous reviewers for positive and constructive comments.

References

1. A. Lacis, J. Hansen, and M. Sato, "Climate forcing by stratospheric aerosols," Geophys. Res. Lett. **19**(15), 1607–1610 (1992).
2. S. Kremser, L. W. Thomason, M. von Hobe, M. Hermann, T. Deshler, C. Timmreck, M. Toohey, A. Stenke, J. P. Schwarz, R. Weigel, S. Fueglistaler, F. J. Prata, J.-P. Vernier, H. Schlager, J. E. Barnes, J.-C. Antuña-Marrero, D. Fairlie, M. Palm, E. Mahieu, J. Notholt, M. Rex, C. Bingen, F. Vanhellemont, A. Bourassa, J. M. C. Plane, D. Klocke, S. A. Carn, L. Clarisse, T. Trickl, R. Neely, A. D. James, L. Rieger, J. C. Wilson, and B. Meland, "Stratospheric aerosol – observations, processes, and impact on climate," Rev. Geophys. **54**(2), 278–335 (2016).
3. J. Hansen, A. Lacis, R. Ruedy, and M. Sato, "Potential climate impact of Mount Pinatubo eruption," Geophys. Res. Lett. **19**(2), 215–218 (1992).
4. J. Hansen, M. Sato, L. Nazarenko, R. Ruedy, A. Lacis, D. Koch, I. Tegen, T. Hall, D. Shindell, B. Santer, P. Stone, T. Novakov, L. Thomason, R. Wang, Y. Wang, D. Jacob, S. Hollandsworth, L. Bishop, J. Logan, A.

Thompson, R. Stolarski, J. Lean, R. Willson, S. Levitus, J. Antonov, N. Rayner, D. Parker, and J. Christy, "Climate forcings in Goddard Institute for Space Studies SI2000 simulations," J. Geophys. Res. **107**(D18), 4347 (2002).
5. M. G. Lawrence, S. Schäfer, H. Muri, V. Scott, A. Oschlies, N. E. Vaughan, O. Boucher, H. Schmidt, J. Haywood, and J. Scheffran, "Evaluating climate geoengineering proposals in the context of the Paris Agreement temperature goals," Nat. Commun. **9**(1), 3734 (2018).
6. M. P. McCormick, P. Hamill, W. P. Chu, T. J. Swissler, L. R. McMaster, and T. J. Pepin, "Satellite studies of the stratospheric aerosol," Bull. Am. Meteorol. Soc. **60**(9), 1038–1046 (1979).
7. L. W. Thomason, L. R. Poole, and T. Deshler, "A global climatology of stratospheric aerosol surface area density deduced from Stratospheric Aerosol and Gas Experiment II measurements: 1984-1994," J. Geophys. Res. D Atmospheres **102**(D7), 8967–8976 (1997).
8. L. A. Rieger, A. E. Bourassa, and D. A. Degenstein, "Stratospheric aerosol particle size information in Odin-OSIRIS limb scatter spectra," Atmos. Meas. Tech. **7**(2), 507–522 (2014).
9. L. D. Travis, "Remote sensing of aerosols with the Earth Observing System Polarimeter," Proc. SPIE **1747**, 154–164 (1992).
10. L. Travis, "Earth Observing System Polarimeter," in J. Hansen, W. Rossow, and I. Fung, editors, *Long-Term Monitoring of Global Climate Forcings and Feedbacks*, NASA CP-3234, 40–46 (1993).
11. J. Hansen, W. Rossow, B. Carlson, A. Lacis, L. Travis, A. Del Genio, I. Fung, B. Cairns, M. Mishchenko, and M. Sato, "Low-cost long-term monitoring of global climate forcings and feedbacks," Clim. Change **31**(2-4), 247–271 (1995).
12. M. I. Mishchenko, B. Cairns, G. Kopp, C. F. Schueler, B. A. Fafaul, J. E. Hansen, R. J. Hooker, T. Itchkawich, H. B. Maring, and L. D. Travis, "Accurate monitoring of terrestrial aerosol and total solar irradiance: introducing the Glory Mission," Bull. Am. Meteorol. Soc. **88**(5), 677–692 (2007).
13. D. Tanré, F. M. Bréon, J. L. Deuzé, O. Dubovik, F. Ducos, P. François, P. Goloub, M. Herman, A. Lifermann, and F. Waquet, "Remote sensing of aerosols by using polarized, directionnal and spectral measurements within the A-Train: the PARASOL mission," Atmos. Meas. Tech. **4**(7), 1383–1395 (2011).
14. B. Fougnie, T. Marbach, A. Lacan, R. Lang, P. Schlüssel, G. Poli, R. Munro, and A. B. Couto, "The multi-viewing multi-channel multi-polarisation imager – overview of the 3MI polarimetric mission for aerosol and cloud characterization," J. Quant. Spectrosc. Radiat. Transf. **219**, 23–32 (2018).
15. *Thriving on Our Changing Planet: A Decadal Strategy for Earth Observation from Space* (National Academies, 2018).
16. O. Dubovik, Z. Li, M. I. Mishchenko, D. Tanre, Y. Karol, B. Bojkov, B. Cairns, D. J. Diner, R. Espinosa, P. Goloub, X. Gu, O. Hasekamp, J. Hong, W. Hou, K. D. Knobelspiesse, J. Landgraf, L. Li, P. Litvinov, Y. Liu, A. Lopatin, T. Marbach, H. Maring, V. Martins, Y. Meijer, G. Milinevsky, S. Mukai, F. Parol, Y. Qiao, L. Remer, J. Rietjens, I. Sano, P. Stammes, S. Stamnes, X. Sun, P. Tabary, L. D. Travis, F. Waquet, F. Xu, C. Yan, and D. Yin, "Polarimetric remote sensing of atmospheric aerosols: instruments, methodologies, results, and perspectives," J. Quant. Spectrosc. Radiat. Transf. **224**, 474–511 (2019).
17. B.-C. Gao and Y. J. Kaufman, "Selection of the 1.375-μm channel for remote sensing of cirrus clouds and stratospheric aerosols from space," J. Atmos. Sci. **52**(23), 4231–4237 (1995).
18. M. I. Mishchenko and L. D. Travis, "Satellite retrieval of aerosol properties over the ocean using polarization as well as intensity of reflected sunlight," J. Geophys. Res. **102**(D14), 16989–17013 (1997).
19. M. I. Mishchenko and L. D. Travis, "Satellite retrieval of aerosol properties over the ocean using measurements of reflected sunlight: effect of instrumental errors and aerosol absorption," J. Geophys. Res. **102**(D12), 13543–13553 (1997).
20. M. I. Mishchenko, L. D. Travis, W. B. Rossow, B. Cairns, B. E. Carlson, and Q. Han, "Retrieving CCN column density from single-channel measurements of reflected sunlight over the ocean: a sensitivity study," Geophys. Res. Lett. **24**(21), 2655–2658 (1997).
21. M. I. Mishchenko, L. D. Travis, and A. A. Lacis, *Multiple Scattering of Light by Particles: Radiative Transfer and Coherent Backscattering* (Cambridge University, 2006). https://www.giss.nasa.gov/staff/mmishchenko/publications/Book3.pdf
22. M. I. Mishchenko, *Electromagnetic Scattering by Particles and Particle Groups: An Introduction* (Cambridge University, 2014). https://www.giss.nasa.gov/staff/mmishchenko/publications/Book_4.pdf
23. J. E. Hansen, "Circular polarization of sunlight reflected by clouds," J. Atmos. Sci. **28**(8), 1515–1516 (1971).
24. M. I. Mishchenko, "The fast invariant imbedding method for polarized light: computational aspects and numerical results for Rayleigh scattering," J. Quant. Spectrosc. Radiat. Transf. **43**(2), 163–171 (1990).
25. M. I. Mishchenko, L. D. Travis, and A. A. Lacis, *Scattering, Absorption, and Emission of Light by Small Particles* (Cambridge University, 2002). https://www.giss.nasa.gov/staff/mmishchenko/books.html
26. J. E. Hansen and L. D. Travis, "Light scattering in planetary atmospheres," Space Sci. Rev. **16**(4), 527–610 (1974).
27. R. J. Peralta, C. Nardell, B. Cairns, E. E. Russell, L. D. Travis, M. I. Mishchenko, B. A. Fafaul, and R. J. Hooker, "Aerosol Polarimetry Sensor for the Glory Mission," Proc. SPIE **6786**, 67865L (2007).
28. P.-Y. Deschamps, F. M. Bréon, M. Leroy, A. Podaire, A. Bricaud, J.-C. Buriez, and G. Seze, "The POLDER mission: instrument characteristics and scientific objectives," IEEE Trans. Geosci. Remote Sens. **32**(3), 598–615 (1994).

29. S. Bouffiès, F. M. Bréon, D. Tanré, and P. Dubuisson, "Atmospheric water vapor estimate by a differential absorption technique with the polarisation and directionality of the Earth reflectances (POLDER) instrument," J. Geophys. Res. **102**(D3), 3831–3841 (1997).
30. Y. Iwasaka and S. Hayashida, "The effects of the volcanic eruption of St. Helens on the polarization properties of stratospheric aerosols: lidar measurement at Nagoya," J. Meteorol. Soc. Jpn. **59**(4), 611–614 (1981).
31. Y. Iwasaka, "Measurement of depolarization of stratospheric particles by lidar – a case study on the disturbed stratospheric aerosol layer by the volcanic eruption of Mt. El Chichon," J. Geomag. Geoelectr. **38**(8), 729–740 (1986).
32. D. M. Winker and M. T. Osborn, "Preliminary analysis of observations of the Pinatubo volcanic plume with a polarization-sensitive lidar," Geophys. Res. Lett. **19**(2), 171–174 (1992).
33. C. Flesia, A. Mugnai, Y. Emery, S. Godin, L. de Schoulepnikoff, and V. Mitev, "Interpretation of lidar depolarization measurements of the Pinatubo stratospheric aerosol layer during EASOE," Geophys. Res. Lett. **21**(13), 1443–1446 (1994).
34. A. Hoffmann, C. Ritter, M. Stock, M. Maturilli, S. Eckhardt, A. Herber, and R. Neuber, "Lidar measurements of the Kasatochi aerosol plume in August and September 2008 in Ny-Ålesund, Spitsbergen," J. Geophys. Res. **115**, D00L12 (2010).
35. A. Ansmann, M. Tesche, S. Groß, V. Freudenthaler, P. Seifert, A. Hiebsch, J. Schmidt, U. Wandinger, I. Mattis, D. Müller, and M. Wiegner, "The 16 April 2010 major volcanic ash plume over central Europe: EARLINET lidar and AERONET photometer observations at Leipzig and Munich, Germany," Geophys. Res. Lett. **37**(13), 13810 (2010).
36. S. Groß, V. Freudenthaler, M. Wiegner, J. Gasteiger, A. Geiß, and F. Schnell, "Dual-wavelength linear depolarization ratio of volcanic aerosols: lidar measurements of the EyjafjallajOkull plume over Maisach, Germany," Atmos. Environ. **48**, 85–96 (2012).
37. D. M. Winker, Z. Liu, A. Omar, J. Tackett, and D. Fairlie, "CALIOP observations of the transport of ash from the Eyjafjallajökull volcano in April 2010," J. Geophys. Res. **117**(D20), D00U15 (2012).
38. Y. M. Noh, D. H. Shin, and D. Müller, "Variation of the vertical distribution of Nabro volcano aerosol layers in the stratosphere observed by LIDAR," Atmos. Environ. **154**, 1–8 (2017).
39. M. I. Mishchenko, L. D. Travis, R. A. Kahn, and R. A. West, "Modeling phase functions for dustlike tropospheric aerosols using a shape mixture of randomly oriented polydisperse spheroids," J. Geophys. Res. **102**(D14), 16831–16847 (1997).
40. O. Dubovik, A. Sinyuk, T. Lapyonok, B. N. Holben, M. Mishchenko, P. Yang, T. F. Eck, H. Volten, O. Muñoz, B. Veihelmann, W. J. van der Zande, J.-F. Leon, M. Sorokin, and I. Slutsker, "Application of spheroid models to account for aerosol particle nonsphericity in remote sensing of desert dust," J. Geophys. Res. **111**(D11), D11208 (2006).
41. L. Bi, P. Yang, G. W. Kattawar, and M. I. Mishchenko, "Efficient implementation of the invariant imbedding T-matrix method and the separation of variables method applied to large nonspherical inhomogeneous particles," J. Quant. Spectrosc. Radiat. Transf. **116**, 169–183 (2013).
42. D. L. Coffeen and J. E. Hansen, "Polarization studies of planetary atmospheres," in *Planets, Stars and Nebulae Studied with Photopolarimetry*, T. Gehrels, ed. (University of Arizona, 1974), pp. 518–581.
43. G. Milinevsky, Ya. Yatskiv, O. Degtyaryov, I. Syniavskyi, M. Mishchenko, V. Rosenbush, Yu. Ivanov, A. Makarov, A. Bovchaliuk, V. Danylevsky, M. Sosonkin, S. Moskalov, V. Bovchaliuk, A. Lukenyuk, A. Shymkiv, and E. Udodov, "New satellite project Aerosol-UA: remote sensing of aerosols in the terrestrial atmosphere," Acta Astronaut. **123**, 292–300 (2016).
44. P. Davidson, C. Burgoyne, H. Hunt, and M. Causier, "Lifting options for stratospheric aerosol geoengineering: advantages of tethered balloon systems," Philos Trans A Math Phys Eng Sci **370**(1974), 4263–4300 (2012).
45. A. Robock, "Stratospheric aerosol geoengineering," Iss. Environ. Sci. Technol. **38**, 162–185 (2014).
46. D. G. MacMartin, B. Kravitz, S. Tilmes, J. H. Richter, M. J. Mills, J.-F. Lamarque, J. J. Tribbia, and F. Vitt, "The climate response to stratospheric aerosol geoengineering can be tailored using multiple injection locations," J. Geophys. Res. Atmos. **122**(23), 12574–12590 (2017).
47. W. Smith and G. Wagner, "Stratospheric aerosol injection tactics and costs in the first 15 years of deployment," Environ. Res. Lett. **13**(12), 124001 (2018).
48. D. W. Keith, "Photophoretic levitation of engineered aerosols for geoengineering," Proc. Natl. Acad. Sci. U.S.A. **107**(38), 16428–16431 (2010).
49. D. K. Weisenstein, D. W. Keith, and J. A. Dykema, "Solar geoengineering using solid aerosol in the stratosphere," Atmos. Chem. Phys. **15**(20), 11835–11859 (2015).
50. A. J. Ferraro, A. J. Charlton-Perez, and E. J. Highwood, "Stratospheric dynamics and midlatitude jets under geoengineering with space mirrors and sulfate and titania aerosols," J. Geophys. Res. Atmos. **120**(2), 414–429 (2015).